

The Effect of Friction Stir Processing Speed Ratio on the Microstructure and Mechanical Properties of A 430 Ferritic Stainless Steel

A. Salemi Golezani^{a,*}, S. M. Arab^a, Sh. Javadi^a, F. Kargar^b

^a Department of Materials Engineering, Islamic Azad University - Karaj Branch, Karaj, Iran.

^b Department of Materials Engineering, Tarbiat Modares University, Tehran, Iran.

ARTICLE INFO

Article history:

Received 17 Nov. 2013

Accepted 14 Mar. 2014

Available online 15 May 2014

Keywords:

Friction stir welding

A 430 ferritic stainless steel

Welding speed

ABSTRACT

This study is an attempt to investigate the effect of welding rotational and traverse speed on mechanical and microstructural properties of A 430 stainless steel in order to give an effective processing window to achieve appropriate microstructure and mechanical properties. There are a wide range of industrial uses for ferritic stainless steel. Since they have some problems like grain coarsening and martensitic transformation during conventional fusion welding, solid state welding methods have found a great interest. A heavy duty NC machine is used for FSW. Water cooled brass chamber is used to prevent the tool from severe wear and damage. In order to study the effect of rotational to welding speed ratio ($\vartheta = w(\text{rpm})/v(\text{mm}/\text{min})$) on microstructure, rotational speeds of 600,800 rpm and welding speeds of 50, 100, 150, and 200 mm/min with a spindle tilt angle of 3° were selected. Results showed that ferrite grain size decreased by increasing the welding speed at constant rotational speeds, which proves dynamic recrystallization occurrence in the nugget zone. Mechanical tests showed that the strength and hardness of the weld zone increased compared to the base metal.

1. Introduction

Although fusion welding methods are still used for bonding of various metallic products, because of their metallurgical problems, solid state welding processes like friction stir welding (FSW), forge welding, pressure welding, ultrasonic welding etc have been developed during recent years [1]. In the FSW which is invented in TWI of UK in 1991, an inconsumable rotating tool containing pin and shoulder, is inserted into a seam between two

flat sheets and welds them via frictional heating created by shoulder and severe plastic deformation due to stirring the material around the pin [2-3]. Some of most important parameters of FSW are tool geometry [ref. 4-6], target depth and spindle tilt angle [2, 3], and rotating and traverse speed [2] which have considerable effects on microstructure and mechanical properties of weldment [7]. FSW includes three main welding zones with different metallurgical structures and heat input

Corresponding author:

E-mail address: salemiali@kiauo.ac.ir (Ali Salemi Golezani).

rates. These three zones are Stirred Zone (SZ) with high temperature range and material flow, Thermo Mechanically Affected Zone (TMAZ) with medium temperature range and material flow, and Heat Affected Zone (HAZ) with medium temperature range and without material flow, respectively [2]. Ferritic stainless steels are Fe-C-Cr alloys with 12-30% of Chromium and have ferritic structure (α -ferrite with BCC crystallographic structure) at room temperature. Although they are cheaper than other grades of stainless steels and more corrosion resistant, they have less workability and more susceptibility to cracking [8]. AISI 430 is one of the most applied stainless steels and is non-heat treatable. It is used for nitric acid storage tanks, tempering baskets, and decorative components [9]. Due to the stainless steels fusion welding limitations like grain growth and formation of martensite phase [9], FSW has been carried out on them because of no melting problems, less microstructure changes and higher efficiency. Numerous researchers have studied friction stir welding of stainless steels up to now [10-25]. Cho and et al. [10] studied the microstructure of FSWed 409 ferritic stainless steel.

They observed fine grained structure and high fraction of low angle grain boundaries in the stirred zone as compared to that in the base metal. A microstructural study showed acicular shaped bainitic ferrite in most parts of the stirred zone in a FSWed ferritic stainless steel in addition to observed shear texture [11]. Equiaxed grain structure due to dynamic recrystallization with no Cr carbides in the stirred zone and heat affected zone of a FSWed 409L ferritic stainless steel was observed [12]. Also, coarse grain ferrite-martensite structure in the FSWed A409 ferritic stainless steel due to the rapid cooling rate and high strain induced by severe plastic deformation caused by frictional stirring has been observed. This duplex structure causes higher tensile strength and hardness of the weld metal [13]. It is also seen that an increase in traverse speed or decrease in the rotational speed can lead to an ultra fine grain structure and higher mechanical properties. On the other hand, it can cause groove-like defects due to insufficient heat input [14, 15]. M. B. Bilgin and et al. [16]

observed no sigma phase presence and excessive grain growth during FSW of an A 430 ferritic stainless steel. They also showed that the impact energy of the weld metal decreased by increasing the tool rotational speed and decreasing traverse speed.

This study is an attempt to investigate the effect of welding rotational and traverse speed on mechanical and microstructural properties of A 430 stainless steel in order to give an effective processing window to achieve appropriate microstructure and mechanical properties.

2. Experimental

The AISI A430 stainless steel with chemical composition (wt-%) of Fe-0.004C-16.225Cr-0.533Si-0.524Mn-0.145Ni was machined to sheets with a dimension of $10 \times 30 \times 2$ mm³. A heavy duty NC machine was used for FSW. Water cooled brass chamber was used to prevent the tool from severe wear and damage. Argon gas protection was applied to protect the tool against high temperature oxidation. A 16mm-diameter cylindrical tool with a threadless truncated cone pin was made from tungsten carbide. In order to study the effect of rotational to welding speed ratio ($\vartheta = w(\text{rpm})/v(\text{mm}/\text{min})$) on microstructure, rotational speeds of 600 and 800 rpm and welding speeds of 50, 100, 150, and 200 mm/min with a spindle tilt angle of 3° were selected. The samples were cleaned by acetone before welding to remove the surface contaminants. For welding, at first the rotating tool penetrated 1.8mm into the sample, held for seconds to heat it up and then traversed along the rolling direction. After preparing the proper samples from welded sheets and etching by picric acid etchant for 2 min, OM and SEM examinations were carried out to study the FSW parameters effect on microstructure. Longitudinal and vertical tensile tests based on AWS B4 were carried out by Instron-5500R tensile test machine in the tension speed of 5mm/min. Vickers micro-hardness measurements were carried out across the welds and perpendicular to the welding direction using a Buehler micro-hardness tester with a load of 100 Kgf (~980 N) and dwell time of 12 s.

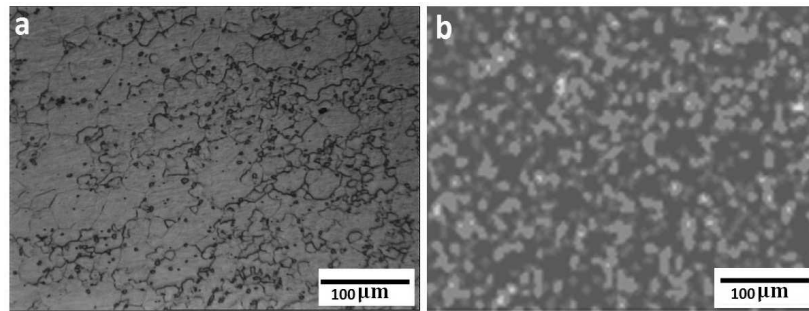


Fig. 1. a) Microstructure of the used stainless steel, b) X-ray distribution map of carbides (white spots)

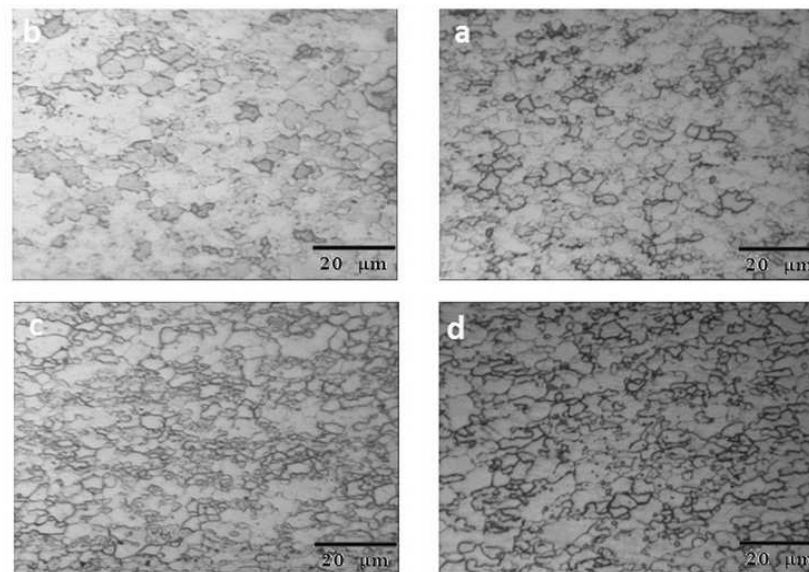


Fig. 2. Stirred zone microstructure of specimens by $\omega = 600rpm$, a) $50mm/min$, b) $100mm/min$, c) $150mm/min$, and d) $200mm/min$ welding speeds

3. Results and Discussion

Fig 1a illustrates the ferritic microstructure containing chromium carbides particles and fig 1b shows the X-ray map distribution of carbides in the matrix. The mean grain size of the matrix ferrite was $26 \mu m$ and the mean particles size was $0.8 \mu m$.

Fig 2 shows the microstructure of stirred zone for $\omega = 600rpm$ and different traverse speeds. Microstructure contains ferrite and inhomogeneous distributed carbides. This structure was also seen in the stirred zone of $\omega = 800rpm$ specimens (figure 3). Microstructure examination showed that carbides size in the stir zone remained constant approximately.

Carbides particle distribution also remained approximately unchanged (fig 4). This can be

related to homogenous plastic deformation in the stirred zone which has led to uniform rearrangement of particles [2]. Fig 5a illustrates the mean ferrite grain size of SZ in the samples with different speeds. It shows that although the grain size decreased by increasing the welding speed, there was no remarkable difference in the grain size in the different zones of the weld. The grain size of advancing and retreating sides was identical. It can be related to the simultaneous higher strain rate and temperature in the advancing and lower strain rate and temperature in the retreating sides which counteract each other effect on grain refinement.

Higher stacking fault energy of AISI 430 to austenitic stainless steels leads to more grain refining chance due to dynamic recrystallization

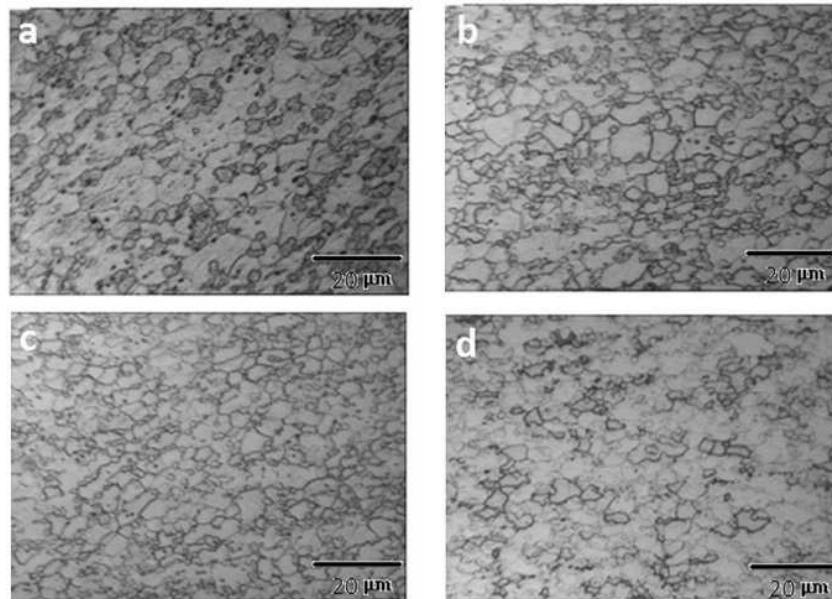


Fig. 3. Stirred zone microstructure of specimens by $\omega = 800\text{rpm}$, a) $50\text{mm}/\text{min}$, b) $100\text{mm}/\text{min}$, c) $150\text{mm}/\text{min}$ and d) $200\text{mm}/\text{min}$ welding speeds

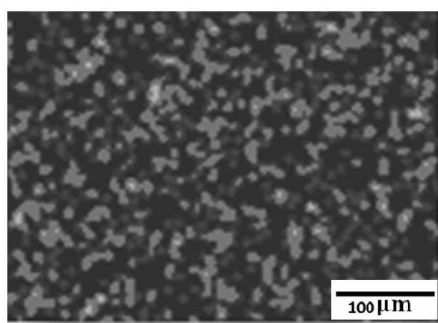


Fig. 4. X-ray distribution map of carbides (white spots) for $\vartheta = 600/200$ specimen

[26]. Other studies have also showed that increasing the welding speed increases the strain rate and higher strain rates usually lead to lower grain size. Higher strain rates enhance the Zener-Hollomon parameter (Z-H), which is the relationship between the temperature and strain rate in thermo mechanical processes. Higher Z-H parameter cause to lower grain size based on equation (1) [27]:

$$d = (a + b \ln Z)^{-1} \quad [1]$$

Where d is mean grain size, and a and b are constant. Increasing the rotational speed leads to heat input increase, Z-H reduction and finally grain size enhancement. Fig 5b shows the ferrite grain size of TMAZ in samples with different welding speeds. Grains of TMAZ are

bigger than SZ because of incomplete dynamic recrystallization. Carbide particle size in TMAZ was also

enlarged because of deformation speed reduction [28]. Fig 6 shows the carbides distribution of for $\vartheta = 600/200$ specimen in TMAZ. Another important microstructural event which has happened in the FSWed AISI 430 is sigma-phase formation. Because of higher temperature due to higher heat input, its formation is more likely in the higher rotational and lower traverse speeds. Because of small grains in the SZ, Cr atoms can diffuse through the boundaries and form the sigma-phase [29]. Sigma-phase enhances the tensile strength at higher temperature and reduces the ductility. Fig 7a illustrates the SEM image of SZ for $\vartheta = 800/50$ specimen. It shows no sigma-phases, but EDAX analysis (fig 7b) confirms their presence as black spots in fig 7a. Although it seems to be necessary to use TEM to make sure of sigma phase precipitation, there is possibility for its formation because of severe plastic deformation [30]. When there is severe plastic deformation, ferrite to austenite and then to martensite is possible [31]. Fig 8 shows no martensite in the microstructure of $\vartheta = 600/50$ and $\vartheta = 800/200$ specimens.

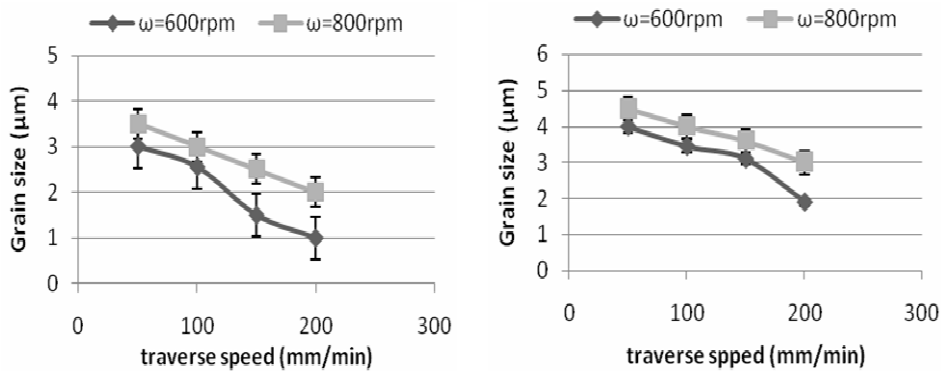


Fig. 5. Ferrite grain size of a SZ and b TMZA in samples with different welding and rotational speeds.

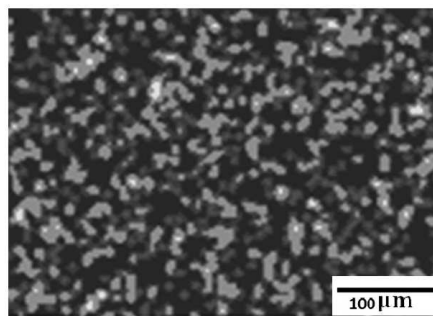


Fig. 6. X-ray distribution map of carbides in TMAZ (white spots) for $\vartheta = 600/200$ specimen

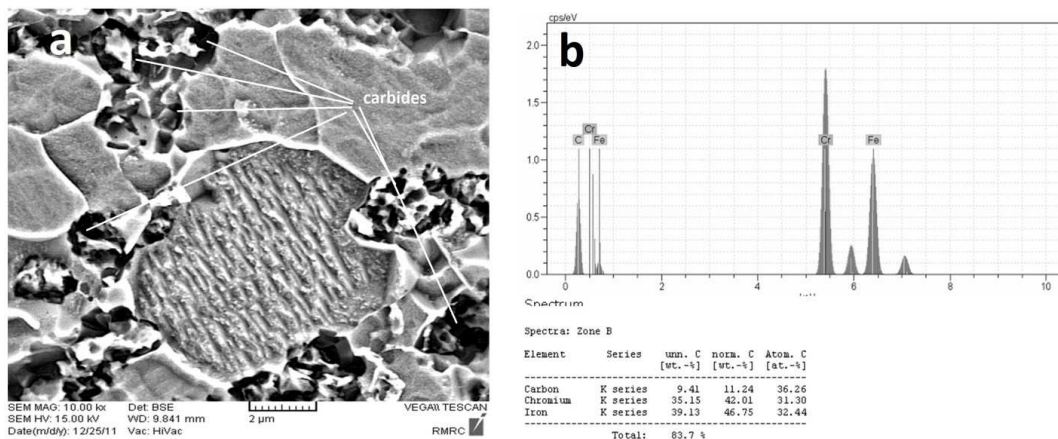


Fig. 7. a) SEM image of stirred zone in $\vartheta = 800/50$ specimen and b) EDAX pattern

After EDAX analysis of the white spots, it is confirmed that they are chromium carbide (Figs 8b, c, and d).

Tensile test for the as received material showed tensile strength of 510 MPa and yield strength of 360MPa. Elongation was about 33%. Because all transverse specimens failed in the base metal, the main attention was given to the longitudinal specimens.

Fig 9a shows the yield strength of transverse specimens. As can be seen, all samples show an

enhancement in the yield strength which is related to grain refining [32].

Carbide particles size did not have a remarkable effect because their size remained unchanged in comparison with the base metal. Fig 9b also shows the tensile strength of transverse specimens with different FSW speed ratios. It is expected to have higher tensile strength through more grain refinement due to higher traverse speeds, but there was no noticeable change in the grain size and then in

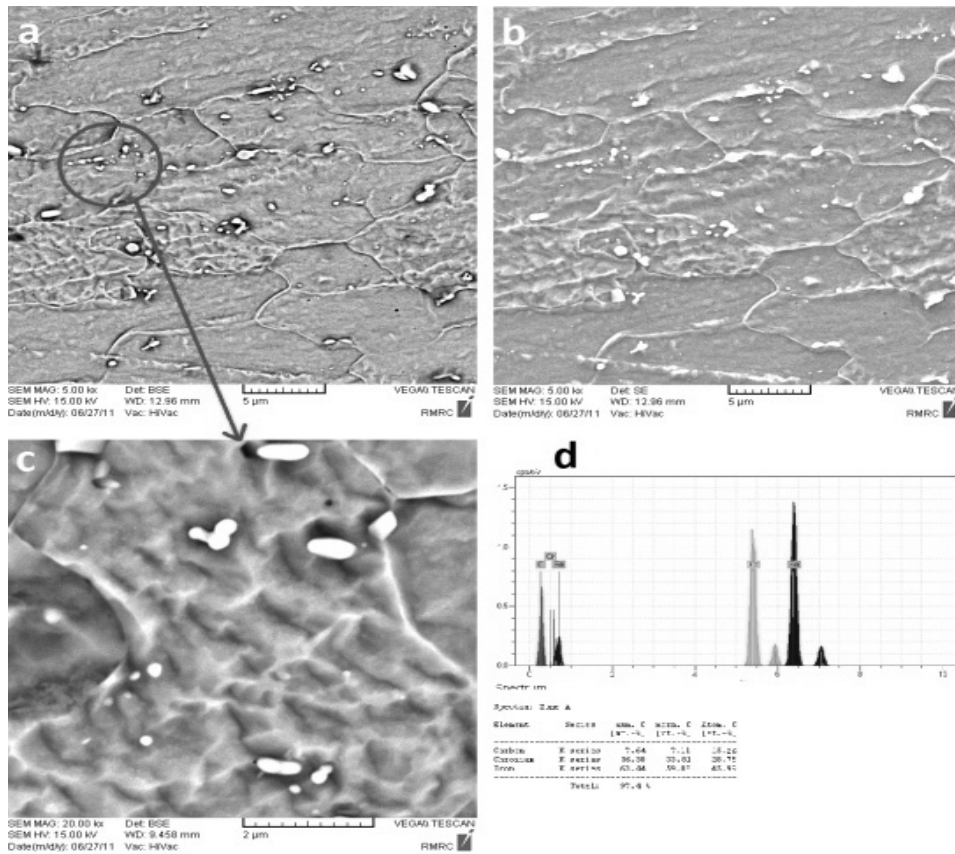


Fig. 8. Microstructure SEM image of a) $\vartheta = 600/50$, b) $\vartheta = 800/200$, c) magnified circle of (a), and d) EDAX analysis of white spots of $\vartheta = 800/200$ specimen

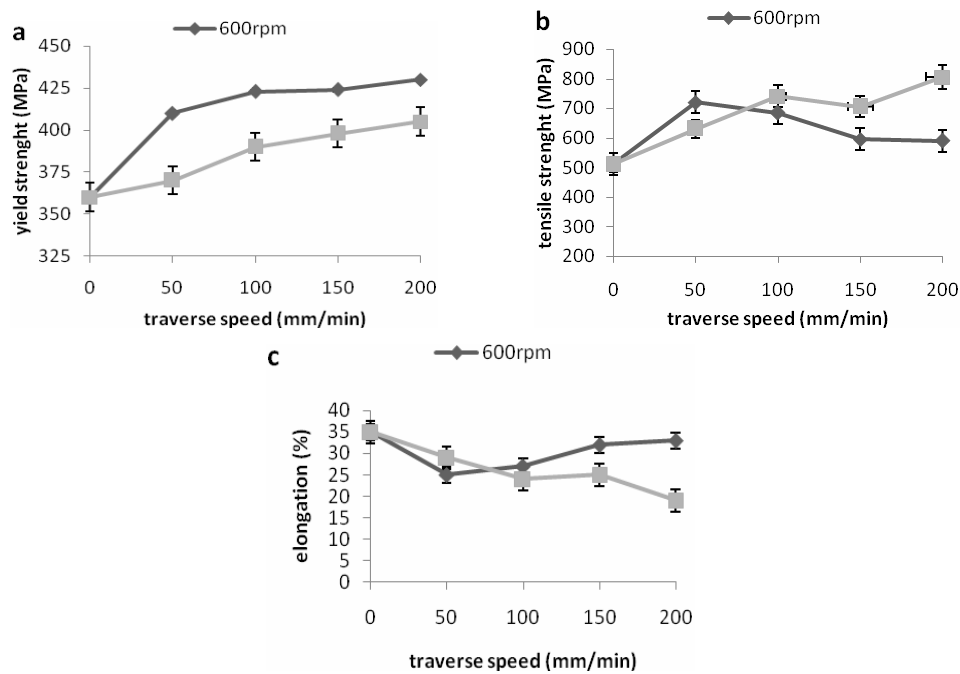


Fig. 9. Comparison of a) yield strength, b) tensile strength, and c) elongation of FSWed specimens by different rotational and welding speeds

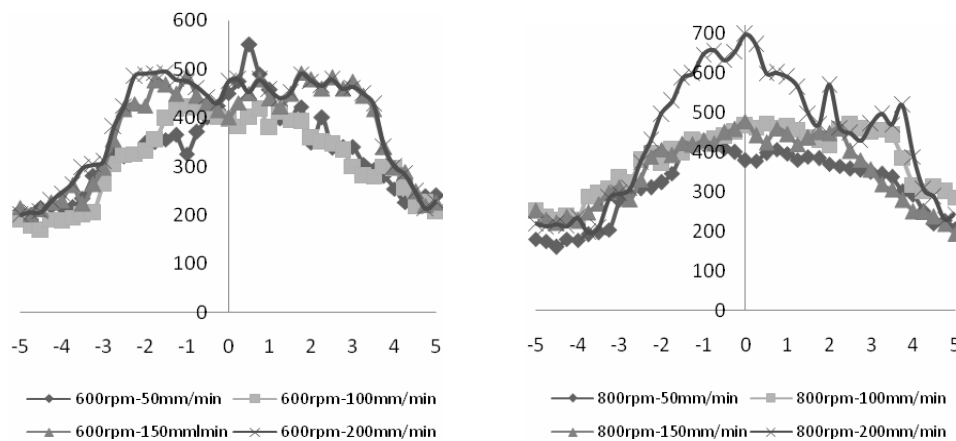


Fig. 10. Hardness profile for a) $\omega = 600rpm$ and b) $\omega = 800rpm$ and different welding speed

tensile strength by welding speed enhancement. Nevertheless, it was seen that tensile strength of $\omega = 800rpm$ increased to about 800MPa from 600MPa when the welding speed rose from 50 mm/min to 200 mm/min. This proved Hall-Petch relationship. It is also observed that tensile strength of $\vartheta = 600/50$ and $600/100$ specimens increases remarkably unlike the $\vartheta = 600/150$ and $600/200$ which showed no significant change because of the tunneling defect.

Fig 9c shows the elongation of different FSWed specimens. As can be seen, elongation values are correlated to their tensile strength reduction. This can be related to work hardening due to grain refinement and its effect on elongation. Figs 10a and 10b illustrate the hardness profile of different FSWed samples. They show an increase in mean hardness of FSWed specimens in comparison with the base metal. This improvement can be attributed to grain refinement of stirred zone. It can also be seen that an increase in welding speed leads to higher hardness due to more grain refinement. Hardness profile's oscillations indicate the layered microstructure of stirred zone. Mean hardness of HAZ remained constant which confirms the grain size stability of this zone after FSW.

4. Conclusions

Microstructural and mechanical examination of FSWed A 430 ferritic stainless steel sheets showed that:

1. Increasing the welding speed in a constant rotational speed decreases the grain size of stirred zone. On the other hand, decreasing the rotational speed in a constant welding speed also reduces the stirred zone grain size. This issue confirms the strain rate and Zener-Hollomon parameter's effect on grain refinement;
2. Sigma-phase precipitants may form more in the high rotational and low welding speeds;
3. Grain size similarity in the advancing and retreating zones of weld can be related to the simultaneous higher strain rate and temperature in the advancing side and lower strain rate and temperature in the retreating side;
4. Grains of TMAZ were bigger than SZ because of incomplete dynamic recrystallization;
5. Elongation reduced and yield strength enhanced as the tensile strength in a constant rotating speed by increasing of traverse speed. Mean hardness of SZ increased in all samples compared to base metal. This can be related to grain refinement in the stirred zone.

References

1. ASM Metals Handbook, Vol. 6, "Welding, Brazing, and Soldering", 2005, USA, ASM International.
2. R. S. Mishra and Z. Y. Ma, "friction stir welding and processing", Mate. Sci. and

- Engineering, R 50, 2005, 1–78.
3. D. Haris and A. F. Nomeran, “Properties of friction Stir welded joints”, TWI Cambridge U.K member, report 726, 2003.
 4. R. Nandan, T. Debroy and H. Bhadeshia, Recent advances in friction-stir welding process, weldment structure and properties, *Mater. Sci.*, 53, 2008, pp. 980-1023.
 5. T. Kheled, “An outsider looks at friction stir welding”, report ANM, 112-n-0506, 2005.
 6. W. M. Thomas, D. G. Staines, I. M. Nomerris and R. DeFrias, “Friction stir welding tools and developments”, The Welding Institute, report TWI Ltd(UK), 2003.
 7. D. Sorensen and T. W. Nelson, “Friction stir welding of ferrous and nickel alloys”, in ASM handbook, vol., “Welding, Brazing, and Soldering”, 111-121, 2007, ASM international.
 8. D. Peckne and I. M. Bernestain, “Handbook of Stainless Steels”, 1997, McGraw-Hill, New York.
 9. B. Leffler, Stainless steels and their properties, *Metall. Trans.*, 31, 2000, 2181- 2192.
 10. H. H. Cho, H. N. Han, S. T. Hong, J. H. Park, Y. J. Kwon, S.H. Kim and R. J. Steel, “Microstructural analysis of friction stir welded ferritic stainless steel”, *Mater. Sci. Eng. A*, 528, 2000, 2889–2894.
 11. H. H. Cho, S. H. Kang, S. H. Kim, K. H. Oh, H. J. Kim, W. S. Chang and H. N. Han, “Microstructural evolution in friction stir welding of high-strength line pipe steel”, *Mater. Design*, 34, 2012, 258–267.
 12. B. W. Ahn, D. H. Choi, D. J. Kim and S. B. Jung, “Microstructures and properties of friction stir welded 409L stainless steel using a Si3N4 tool”, *Mater. Sci. Eng. A*, 532, 2012, 476– 479.
 13. A. K. Lakshminarayanan and V. Balasubramanian, “An assessment of microstructure, hardness, tensile and impact strength of friction stir welded ferritic stainless steel joints”, *Mater. Design*, 31, 2010, 4592–4609.
 14. T. Saeid, A. Abdollah-zadeh, H. Assadi and F. M. Ghaini, “Effect of friction stir welding speed on the microstructure and mechanical properties of a duplex stainless steel”, *Mater. Sci. Eng. A*, 496, 2008, 262–268.
 15. M. Esmailzadeh, M. Shamanian, A. Kermanpur and T. Saeid, “Microstructure and mechanical properties of friction stir welded lean duplex stainless steel”, *Mater. Sci. Eng. A*, 561, 2013, 486–491.
 16. M. B. Bilgin and C. Meran, “The effect of tool rotational and traverse speed on friction stir weldability of AISI 430 ferritic stainless steels”, *Mater. Design*, 33, 2012, 376–383.
 17. Y. C. Chen , H. Fujii, T. Tsumura, Y. Kitagawa, K. Nakata, K. Ikeuchi, K. Matsubayashi, Y. Michishita, Y. Fujiya and J. Katoh, “Banded structure and its distribution in friction stir processing of 316L austenitic stainless steel”, *J. Nuc. Mater.*, 420, 2012, 497–500.
 18. J. Jeon, S. Mironov, Y.S. Sato, H. Kokawa, S.H.C. Park and S. Hirano, “Anisotropy of structural response of single crystal austenitic stainless steel to friction stir welding”, *Acta Mater.*, 61, 2013, 3465–3472.
 19. A. K. Lakshminarayanan and V. Balasubramanian, “Assessment of fatigue life and crack growth resistance of friction stir welded AISI 409M ferritic stainless steel joints”, *Mater. Sci. Eng. A*, 539, 2012, 143–153.
 20. M. Jafarzadegan, A. H. Feng, A. Abdollah-zadeh, T. Saeid, J. Shen and H. Assadi, “Microstructural characterization in dissimilar friction stir welding between 304 stainless steel and St37 steel”, *Mater. Characterization*, 74, 2012, 28-41.
 21. Y. Miyanoa, H. Fuji, Y. Sun, Y. Katada, S. Kuroda and O. Kamiya, “Mechanical properties of friction stir butt welds of high nitrogen-containing austenitic stainless steel”, *Mater. Sci. Eng. A*, 528, 2011, 2917–2921.
 22. M. Jafarzadegan, A. Abdollah-zadeh, A. H. Feng, T. Saeid, J. Shen and H. Assadi, “Microstructure and Mechanical Properties of a Dissimilar Friction Stir Weld between Austenitic Stainless Steel and Low Carbon Steel”, *J. Mater. Sci. Technol.*, 29, (4), 367-372.
 23. Y. S. Sato, T. W. Nelson, C. J. Sterling, R. J. Steel and C. O. Pettersson, “Microstructure

- and mechanical properties of friction stir welded SAF 2507 super duplex stainless steel”, *Mater. Sci Eng. A*, 397, 2005, 376–384.
24. T. Saeid, A. Abdollah-zadeha, T. Shibayanagi, K. Ikeuchi and H. Assadi, “On the formation of grain structure during friction stir welding of duplex stainless steel”, *Mater. Sci Eng. A*, 527, 2010, 6484–6488.
 25. S. H. C. Park, Y. S. Sato, H. Kokawa, K. Okamoto, S. Hirano and M. Inagaki, “Rapid formation of the sigma phase in 304 stainless steel during friction stir welding”, *Scripta Mater.*, 49, 2003, 1175–1180.
 26. H. Kokawa, S. H. C. Park, Y. S. Sato, K. Okamoto, S. Hiranome and M. Inagaki, “Microstructures in friction stir welded 304 austenitic stainless steel”, *Welding in the World*, 49, 2005, 34-40.
 27. ASM Handbook, Vol. 9, “Metallography and Microstructures”, 1992, USA, ASM International.
 28. C. Hamilton, S. Dymek and M. Blicharski, “A model of material flow friction stir welding, *Materials Characterization*”, 59, 2008, 1206-1214.
 29. J. M. Pardal, S. S. M. Tavares, M. C. Fonseca, J. A. de Souza, R. R. A. Côrte and H. F. G. de Abreu, “Influence of the grain size on deleterious phase precipitation in super duplex stainless steel UNS S32750”, *Mater. Characterization*, 60, (3), 2009, 165–172.
 30. E. J. Morley and A. Sandvik, “Heat-affected zone toughness of fsw welded 12%Cr martensitic-ferritic steels”, *Welding J.*, 2003, 431-440.
 31. S. Hwan, C. Park, T. Kumagai, Y. S. Sato and H. Kokawa, “Microstructure and mechanical properties of friction stir welded 430 stainless steel”, *Proc. High Perform. Mater. Symp. on Adv. Welding of Structural Mater. at Seoul, Korea*, 2005, 19-24.
 32. J. J. Zaayman: “Improvements of the mechanical properties of the stir zone in welds of 14 to 17 percent chromium steels”, PhD Thesis, University of Pretoria, 1994.

